Boletim da Sociedade Astronômica Brasileira, **35**, no. 1, 266-267

Astrophysical parameters and evolution of open clusters along the Galactic plane

Thomas M. dos Santos[1], Wagner J. B. Corradi[1,2], Francisco F. S. Maia[4], Filipe A. Ferreira[1], João F. C. Santos Jr.[1], & Mateus S. Angelo[3]

[1] Universidade Federal de Minas Gerais e-mail: thomas.miler.dos.santos@gmail.com, jsantos@fisica.ufmg.br, filipe1906@ufmg.br
[2] Laboratório Nacional de Astrofísica e-mail: wbcorradi@lna.br
[3] Centro Federal de Educação Tecnológica de Minas Gerais e-mail: mateusangelo@cefetmg.br
[4] Universidade Federal do Rio de Janeiro e-mail: ffsmaia@if.ufrj.br

Abstract. Astrometric and photometric data from the Gaia DR3 mission have been used to obtain the astrophysical parameters of 19 objects aged between $6.74 < log[t(years)] < 9.55$. Through the applied methodology, it has been possible to determine central coordinates, parallax, proper motion, membership, age, colour excess, metallicity, distance, tidal radius, and core radius. As the primary outcome, we report, for the first time, the mass value for some open clusters in the sample.

Resumo. Dados astrométricos e fotométricos da missão Gaia DR3 foram utilizados para obter os parâmetros astrofísicos de 19 objetos de idades entre $6.74 < log[t(anos)] < 9.55$. Através da metodologia aplicada foi possível determinar as coordenadas centrais, paralaxe, movimento próprio, pertinência dos membros, idade, avermelhamento, metalicidade, distância, raio de maré e raio de core. Como principal resultado, reportamos de forma inédita o valor de massa para alguns dos aglomerados abertos da amostra.

Keywords. open clusters and associations: general – Galaxy: stellar content – Surveys, mass

1. Introduction

Open clusters play a crucial role in characterizing the Galaxy's disk and are essential to study stellar evolution. Such stellar population units are coeval in terms of age, metallicity, distance, and kinematics but diverse in terms of stellar masses Krumholz, et al. (2019).

As new clusters are discovered and characterized, our understanding of the Galactic structure, its chemical dynamics, and evolution expands significantly.

The cluster sample selected for analysis consists of understudied objects, some of which possess controversial properties, spanning a diverse range of evolutionary stages.

2. Pre-analysis: finding the signature of a cluster

In the first step, we have inspected the dispersion of the data in their Color-Magnitude Diagrams (CMDs) and Vector-Point Diagrams (VPDs) with $G \leq 19 mag$ and $G_{BP} - G_{RP} \leq 2.0$ to identify the overdensities (see 1 on the left) that correspond to stars with similar proper motions and to obtain the central coordinates, proper motion and parallax, as described in Ferreira et al. (2020). In the following, we will use the open cluster Collinder 106 results to exemplify the methodology employed.

With the coordinates of the center (RA and DEC) and proper motion mean values μ_α, μ_δ, we have built a radial density profile (RDP) to estimate the size of each object (1 in the right).

3. CMD Decontamination, isochrone fitting, and structural parameters

To derive membership for the stars, we have applied a routine that evaluates statistically the overdensities of the cluster stars in comparison to those in a nearby field within the 3D astrometric space (μ_α^*, μ_δ and ϖ), as described in Angelo et al. (2019).

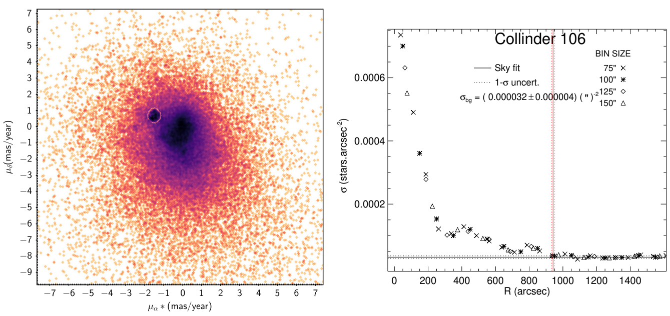

Figure 1. (left) VPD showing an overdensity corresponding to the stars with similar proper motion, that might be assigned as Collinder 106 members. (right) RDP of the selected subsample selected to determine the limiting radius (vertical line).

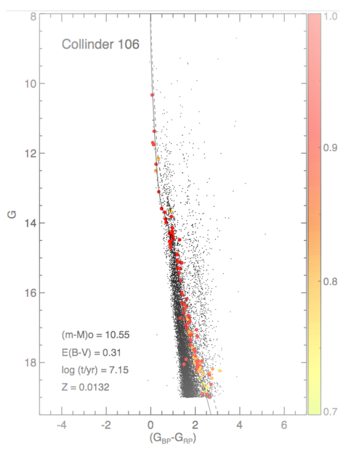

Figure 2. Decontaminated CMD where the colors represent the membership likelihood. The continuous lines are PARSEC isochrones fitted to the data of the cluster.

We have employed solar metallicity PARSEC-COLIBRI models to perform isochrone fittings on the decontaminated

Table 1. Some of the parameters obtained for the nineteen studied clusters.

Cluster	RA (degrees)	DEC (degrees)	μ_α^* (mas/year)	μ_δ (mas/year)	Parallax (mas)	R_t (arcsec)	Number of members
Berkeley 43	288.876	11.269	−1.255	−3.716	0.314	194.959	319
Collinder 106	99.289	6.052	−1.557	0.556	0.618	977.668	116
Collinder 104	99.183	4.994	−1.365	0.610	0.630	–	90
FSR 0123	287.917	12.037	−1.329	−4.198	0.185	1091.666	1002
liu 160	288.897	5.828	−0.187	−4.628	0.471	616.666	77
liu 461	286.796	11.463	−2.00	−4.541	0.236	350.000	66
NGC 2301	102.932	0.445	−1.356	−2.184	1.155	998.840	524
NGC 5460	211.784	−48.263	−6.637	−3.392	1.403	2188.965	124
NGC 6231	253.561	−41.832	−0.605	−2.158	0.618	7388.049	1137
NGC 6709	282.830	10.320	1.443	−3.540	0.940	2104.392	233
Sim 51	283.231	8.214	−1.254	−3.849	0.880	1462.500	185
Sim 53	290.489	9.067	0.701	−3.426	1.143	2425.000	192
Sim 54	288.531	14.281	2.438	1.080	1.648	2737.500	147
Sim 55	286.104	15.882	−0.573	−5.880	1.200	1562.500	85
UBC 118	282.667	9.746	−0.259	−4.201	0.573	558.333	143
UBC 120	284.109	13.254	1.066	1.424	0.811	520.833	43
UFMG 26	288.903	12.846	−1.250	−3.473	0.500	587.000	160
UFMG 27	287.088	10.175	−0.886	−3.647	0.309	520.833	125
UFMG 62	149.029	−60.183	−5.930	5.173	0.329	533.000	154

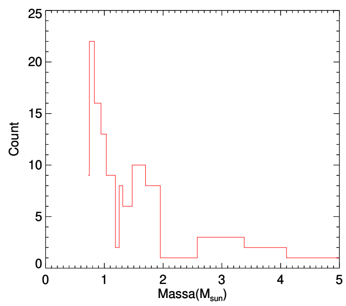

Figure 3. Histogram illustrating the density of different mass values for Collinder 106. The cluster's member stars have masses below 2 solar masses, in their majority.

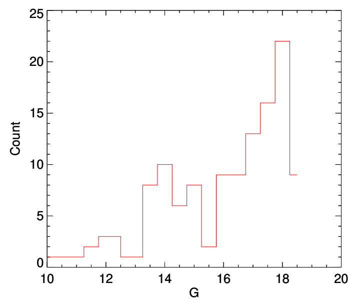

Figure 4. Histogram illustrating the mass distribution of the cluster based on magnitudes. It is evident that the density of stars with low magnitude is higher than the number of stars with high magnitude.

CMD (3) aiming to determine the true distance modulus $(m - M)_0$, $E(B - V)$ colour excess, age ($log(t/yr)$) the metalicities ($[Fe/H]$), for each object.

Structural parameters: core (r_c) and tidal (r_t) radii, have been obtained by King King (1962) model fittings, using a MCMC algorithm.

4. Total Mass

A direct summation of the masses of star members has been made adopting, as the mass of each star, the mass of the nearest point on the fitted isochrone through interpolation routines and the k-nearest neighbors algorithm. The total mass of the cluster has been determined from the integrated magnitude, calculated by summing the flux from member stars, along with the age of the cluster Maia, Piatti, & Santos (2014):

$$\log \mathcal{M} = a + b \log t - 0.4(M_G - M_{G,\odot}) \quad (1)$$

where $a = -6.09$, $b = 0.644$ and $M_{G,\odot} = 4.67$.

When comparing with the astrophysical parameters in the literature, our values show a good agreement, within 0.71% of difference. Some of the results obtained in this work are summarized in Table 1.

5. Conclusions

The mass measurements for the clusters, such as Collinder 104, Collinder 106, and NGC 2301, reveal substantial differences when obtained through different methodologies.

Table 2. Mass difference from the two used methods. M_1 comes from the integrated magnitudes. M_2 results from the sum of member stars

Cluster	M_1 ($M_\odot$)	M_2 ($M_\odot$)	Diff(%)
Collinder 106	21.2	151.4	85
Collinder 104	166.0	143.2	16
NGC 2301	422.2	540.8	22

The analysis has shown discrepancies between the mass values derived from the two distinct methods, as can be seen in 2.

These findings suggest that the integrated magnitudes method may tend to underestimate the cluster's mass, while the computation based on the sum of member stars offers a more accurate approximation of the cluster's visible mass. This clearly illustrates how stars of different masses and magnitudes contribute to the overall mass of the cluster.

Acknowledgements. The authors wish to thank the support of UFMG, LNA, CEFET-MG and UFRJ.

References

Krumholz M. R., McKee C. F., Bland-Hawthorn J., 2019, ARA&A, 57, 227.
Ferreira F. A., Corradi W. J. B., Maia F. F. S., Angelo M. S., Santos J. F. C., 2020, MNRAS, 496, 2021.
Angelo M. S., Santos J. F. C., Corradi W. J. B., Maia F. F. S., 2019, A&A, 624, A8.
King I., 1962, AJ, 67, 471.
Maia F. F. S., Piatti A. E., Santos J. F. C., 2014, MNRAS, 437, 2005.
Babusiaux C., Fabricius C., Khanna S., Muraveva T., Reylé C., Spoto F., Vallenari A., et al., 2023, A&A, 674, A32.